

Three-dimensional resistive metamaterial absorber loaded with metallic resonators for the enhancement of lower-frequency absorption

Yang Shen¹, Jie Qiu Zhang¹, Yong Qiang Pang^{1,2,*}, Lin Zheng¹, Jia Fu Wang¹, Hua Ma¹ and Shao Bo Qu^{1,*}

¹ College of Science, Air Force Engineering University, Xi'an 710051, China; shenyang508@126.com (Y.S.); zhangjiq0@163.com (J.Z.); zhenglin0205@gmail.com (L.Z.); wangjiafu1981@126.com (J.W.); mahuar@163.com (H.M.); Qushaobo@mail.xjtu.edu.cn (S.Q.)

² School of Electronics and Information Engineering, Xi'an Jiaotong University, Xi'an 710049, China; 225pang@163.com (Y.P.)

* Correspondence: 225pang@163.com and Qushaobo@mail.xjtu.edu.cn

Abstract: Resistive patch array incorporating with metallic backplane provided an effective way to the achievement of broadband metamaterial absorbers(MAs). When loading metallic metamaterial to resistive MA, the outstanding construction helps realize more flexible and diversified forms of broadband absorption. In this paper, we attempted to load metallic resonators(MRs) to resistive MA in the three-dimensional construction, which benefits further enhancement of lower-frequency absorption. Simulation showed that the partial absorption band was separated to lower frequency, while the rest of broadband absorption was unaffected. Meanwhile, after combining multi-unit of the proposed MAs, the stair-stepping broadband absorption was also achieved. At last, three samples were fabricated. The agreements between simulations and experimental results demonstrated that resistive MA loaded with MRs provided an effective way for further enhancement of lower-frequency absorption with almost no change of the absorbing structure and areal density. Thus, it is worthy to expect a wide range of applications to emerge inspired from the proposed attempt.

Keywords: metamaterial absorber; metallic resonator; three-dimensional construction; broadband absorption; lower-frequency absorption

1. Introduction

Metamaterials consist of periodic subwavelength unit cell which can provide more possibility to construct the desired constitutive parameters. As new artificial medium, metamaterials have great applications in many fields, such as superlenses [1-3], invisibility cloaks [4-6], and perfect absorbers [7-10]. For the field of electrometric wave absorbing medium, the perfect metamaterial absorber was firstly proposed based on three-layered configuration of metal-dielectric-metal [7]. The strong resonance from the metallic metamaterial and the loss from the dielectric substrate worked together contributing to nearly perfect absorption at one frequency. Based on this, various MAs with one-, two- or multi-band absorption were proposed

[8-13]. However, the highly effective absorption always accompanies with the narrow bandwidth, which was the fundamental obstacle limited the practical application.

To achieve broadband MAs, a lot of attempts were carried out. First of all, the combination of multi-unit exciting contiguous resonances can be thought as a directly way to construct a continuously broadband absorption [14-19]. One the hand, the multi-unit exciting contiguous highly effective absorption peaks can assemble together on the same plane [14,15]. But the inherent contradiction between the absorbing efficiency and the duty ratio always hindered the further enhancement of broadband absorption. On the other hand, the varied units with the contiguous absorption peaks can also be arranged along the wave vector to achieve outstanding broadband absorption [16-18]. But the expansion of absorption bandwidth was carried out at the sacrifice of ultrathin thickness and light weight characteristic. Then, considering the resonance is inspired from the dispersion of effective medium, loading lumped elements to MA can provide an effective way to ameliorate the dispersion relation to achieve broadband absorption [19-22]. More specifically, when loading lumped resistor and capacitor to MA, the several absorption peaks will not only be adjusted to more adjacent frequencies, but they also exhibit low Q factor in the spectrum. And the several absorption peaks with low Q factor finally overlapped together contributing highly effective and broadband absorption. Meanwhile, the materials with strong ohmic loss, such as resistive patch, can also be introduced here to construct broadband MA in electromagnetic wave [23-29]. Compared with the aforementioned MA based on metal-dielectric-metal configuration, resistive MAs were easy to achieve highly effective and broadband absorption as well as other advantages, such as light-weight, low cost, and easy fabrication. However, with deep research of resistive MAs, it was also demonstrated that the further enhancement of broadband absorption, especially for lower-frequency absorption, was not easy to be carried out when the total thickness of the resistive MA was given.

In this paper, aiming at the target of lower-frequency absorption enhancement in resistive MA, we attempted to load MRs to the resistive MA to reconfigure the broadband absorption performance. As a proof, the three-dimensional resistive patch array standing on the metal backplane was firstly introduced here for broadband absorption. Then, the metallic bamboo joint structures as MRs were adhered to the side of resistive patches. The strong resonance inspired by the MRs at lower frequency break the original broadband absorption. Simulation showed that the proposed MA can effectively separate partial absorption band to lower frequency, while keeping the broadband absorption at rest frequencies unchanged. Meanwhile, after combining multi-unit, the stair-stepping broadband absorption was also achieved. At last, three samples were fabricated for experimental demonstration. It was expected that a wide range of applications to emerge inspired from the proposed attempt.

2. Three-dimensional Resistive MA

Using resistive patch to construct broadband MA has always been widely adopted.

Here, our method attempted to using resistive patches to construct array standing up on the metal backplane, the total system can exhibit highly effective and broadband absorption performance. As shown in Figures 1a and 1b, the height, the width and the sheet resistance of each resistive patch were d , a , and fz , respectively. The resistive patch arranged along x -axis direction on the square backplane with the size of p . The accordingly gap between adjacent resistive patches was s . The F4B3 substrate used here as a supporter for the construction of the resistive patch array with height d , width p , and thickness t . The relative permittivity and the loss tangent of the F4B3 substrate were 2.65 and 0.001. The copper plate was used here as backplane with a frequency independent conductivity $\sigma=5.8\times10^7\text{S/m}$ and the thickness $t_c=0.017\text{mm}$. In the simulation, the electric field of the incidence should be set along x -axis, while the magnetic field was along y -axis to obtain the broadband absorption. The absorptive efficiency of the three-dimensional resistive MA under normal incidence can be defined as $A(\omega)=1-R(\omega)-T(\omega)=1-|S_{21}|^2-|S_{11}|^2$, where $A(\omega)$, $|S_{11}|^2$ and $|S_{21}|^2$ are the absorbance, reflectivity and transmissivity, respectively. Due to the existence of metal backplane, the transmission (S_{21}) is zero. Thus, the absorbance can be calculated by $A(\omega) = 1-|S_{11}|^2$ in this paper. After optimization, when the thickness was given as $d=8.0\text{mm}$, the three-dimensional resistive MA can achieve broadband electromagnetic wave absorption with efficiency more than 90% ranging from 4.6 to 21.4GHz, as shown in Figure 1c. Meanwhile, during the optimization process, some parameters of resistive patch array which will affect the broadband absorption performance were also discussed here. As shown in Figures 2a-2d, when increasing the size a of resistive patch from 10.1 to 10.7mm or decreasing the gap s between adjacent resistive patches from 0.9 to 0.3mm, the broadband absorption would further move to lower frequency with very slight extent. The sheet resistance of the resistive patch can be seen as an assistant factor for the improvement of absorption during the operating frequencies. As a comparison, the height of resistive patch played an important role for the enhancement of broadband absorption. With the increase of height from 7.0 to 10.0mm, the low boundary frequency of absorption bandwidth with efficiency more than 90% will further expand from 7.3 to 4.6GHz. Thus, it can be concluded that there was less space for further enhancement of lower-frequency absorption when the height of the three-dimensional resistive MA was given.

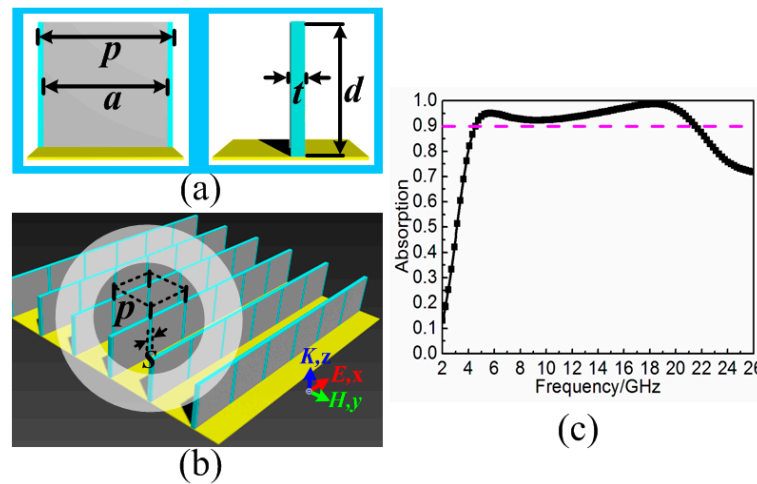


Figure 1. Three-dimensional resistive MA consists of resistive patches and dielectric substrates standing up on the metal backplane. (a) Front view and side view of each unit cell, (b) Perspective view of three-dimensional resistive MA, (c) Absorption spectrum under normal incidence. The optimized parameters of the resistive MA unit cell are given as following: $d=8.0\text{mm}$, $a=10.5\text{mm}$, $s=0.5\text{mm}$, $f_z=75.0\Omega/\text{sq}$, $t=1.0\text{mm}$, and $p=11.0\text{mm}$.

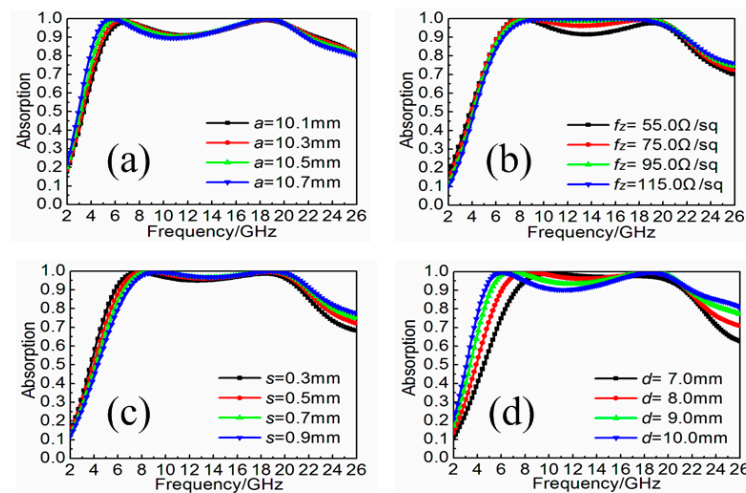


Figure 2. Absorption spectra of the three-dimensional resistive MAs with different (a) size a of resistive patch ranging from 10.1 to 10.7 mm, (b) sheet resistance f_z of resistive patch ranging from 55.0 to 115.0 Ω/sq , (c) gap s between adjacent resistive patches ranging from 0.3 to 0.9 mm, and (d) height d of resistive patch ranging from 7.0 to 10.0 mm.

3. Three-dimensional Resistive MA with MRs

Here, based on the aforementioned design of three-dimensional resistive MA, we attempted to load MRs of bamboo joint structure to reconfigure the broadband absorption performance. The structure diagram was shown in Figure 3a, the F4B3 substrates with height d , width p and thickness t were introduced here to stand up on the squared metal backplane with the size p . On the one side of the substrate, the aforementioned resistive patches were adhered periodically. On the other side of the substrate, metallic bamboo joint structures were also printed accordingly. The height,

the width and the sheet resistance of the resistive patch were d , a , and fz . The width of the wire, width of the bamboo joint, and the gap between adjacent bamboo joints were w , l , and s , respectively. The metallic bamboo joint units were arranged along x -axis with the gap of g above the metal backplane. The electric field of the incidence was also set along x -axis to achieve optimal broadband absorption performance. In the simulation, when the three-dimensional resistive MAs loaded with MRs, the originally continuous broadband absorption performance was not exit. Instead, the partial absorption band was separated to lower frequency. With the increased width l of bamboo joint structures from 2.0 to 6.0mm, the separated absorption band with efficiency more than 90% would gradually move to lower frequencies from 4.0-4.8GHz to 2.3-2.5GHz, while the continuous broadband absorption during higher frequencies was still unaffected, as shown in Figure 4a. Based on the separated broadband absorption performance, a generalized definition of absorption bandwidth was given which reflects the range between the lower boundary frequency of separated absorption band and the upper boundary frequency of unchanged absorption band when the absorption efficiency is more than 90%. Table 1 gave the generalized absorption bandwidth and the corresponding absorption bandwidth ratio for the three-dimensional resistive MAs loaded with different size of MRs. Compared with the former resistive MA in Figure 4b, the absorption bandwidth ratio also had an obvious improvement. With the increased width l of the metallic bamboo joint structure, the absorption bandwidth ratio would further increase. Thus, it is obvious that loading MRs to the three-dimensional resistive MAs provide an alternative way to enhance the lower-frequency absorption we are more concerned and sacrifice partial absorption band in the middle frequencies we are not concerned. Meanwhile, the limited bandwidth ratios of the proposed MA were also calculated based on the theoretical Rozanov limit [30]. During the operating frequency band of 1.0-21.0GHz, the aforementioned three-dimensional resistive MA achieved the limited bandwidth ratio was 0.67. After loading with different sized MRs, the total absorbing efficiency had no obvious change, as given in Figure 4c. Thus, it can be concluded that fundamental absorbing principle is still unchanged during the broad operating frequency band.

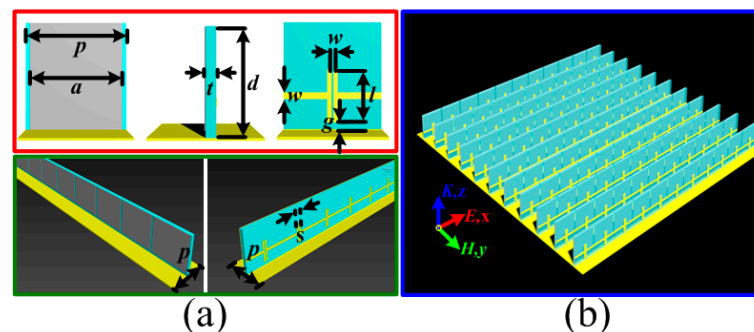


Figure 3. Three-dimensional resistive MAs loaded with MRs. (a) Schematic diagram of the proposed MA unit cell, (b) Perspective view of the proposed MA. The parameters of the proposed MA unit cell are given as following: $d=8.0\text{mm}$, $a=10.5\text{mm}$, $s=0.5\text{mm}$, $fz=75.0\Omega/\text{sq}$, $p=11.0\text{mm}$, $t=1.0\text{mm}$, $w=0.5\text{mm}$, and $s=0.5\text{mm}$.

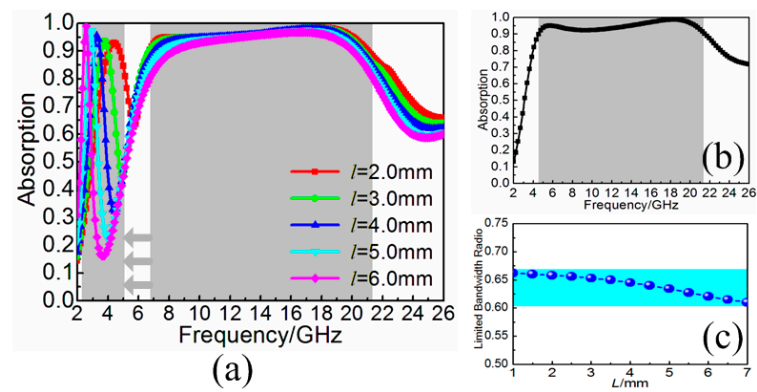


Figure 4. (a) Absorption spectrum of the three-dimensional resistive MAs loaded with different width l of MRs. (b) Absorption spectrum of the three-dimensional resistive MA. (c) Limited bandwidth ratio of the proposed MA with different width l of metallic bamboo joint structure.

Table 1. Calculated absorption bandwidth ratio of the three-dimensional resistive MAs loaded with different width l of metallic bamboo joint structure.

l (mm)	Absorption bandwidth(GHz)	Absorption bandwidth ratio
2.0	4.0-21.1	1:5.3
3.0	3.5-20.7	1:5.9
4.0	3.1-20.6	1:6.6
5.0	2.7-20.3	1:7.5
6.0	2.4-20.0	1:8.3
7.0	2.3-19.8	1:8.6

Note: l : the width of the loaded metallic bamboo joint structure; Absorption bandwidth: a generalized concept reflects the range between lower boundary frequency of separated absorption band and the upper boundary frequency of unchanged absorption band when the absorption efficiency is more than 90%. Absorption bandwidth ratio: a normalized ratio between the upper boundary frequency and lower boundary frequency.

To explore the absorption principle of the proposed MA, the electric field intensity distributions and surface current distributions of the proposed MA with different size of MRs were given in Figure 5. From the distributions on the upper, it was obvious that the induced electric field on the three models were all obviously enhanced at the gap of bamboo joint structure. The corresponding surface current distributions on the below also indicated that much induced surface current was generated at the gap of the metallic bamboo joint structure. The metallic bamboo joint structures just like electric resonators which generated resonance at certain frequency under normal incidence. Based on this, the metallic bamboo joint structure can be seen as simple *RLC* series circuit. And the width l of the bamboo joint was seen as a great factor which will influence the equivalent capacitance C and then determined the resonance frequency. Therefore, the width l of the bamboo joint has always been seen as a vital parameter directly determined the separated absorption. Meanwhile, as new artificial medium, the constitutive parameters of the proposed MA and its components were worthy to be discussed here to further principle analysis[19]. Figure

6a firstly gave the equivalent permittivity and permeability of the three-dimensional resistive MA. Due to the low conductivity characteristic of the resistive patch, the resistive MA possessed flat dispersion curve, especially nearly constant in the shaded region. Figure 6b gave the equivalent permittivity and permeability of the metallic bamboo joint structure printed on the F4B3 substrate. Due to the existence of the gap in the metallic unit cell, there was strong resonance in dispersion curve at lower frequency in the shaded region. When the three-dimensional resistive MAs with the flat dispersion curve and the MRs with the strong resonance were combined together, the strong resonance at the lower frequency and the flat dispersion were all retained as shown in Figure 6c. Thus, based on the discussion aforementioned, it is worthy to be noted that our attempt effectively enhanced the lower-frequency absorption we are particularly concerned as well as have no influence on the broadband absorption during the rest frequencies. Meanwhile, it also retains the original advantages of simple absorbing structure and light-weight characteristic.

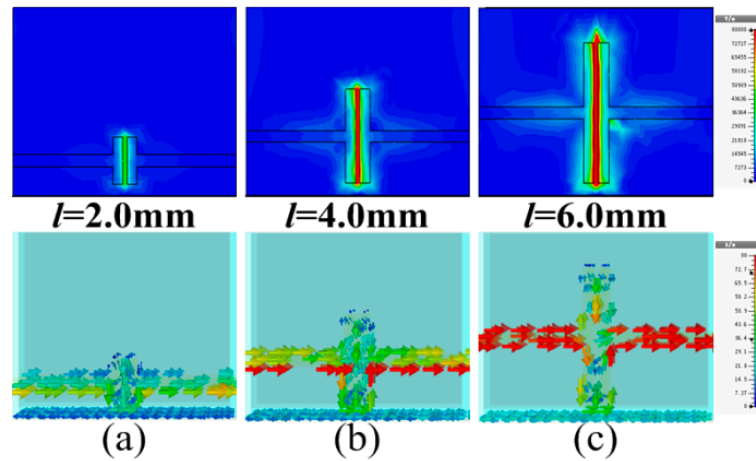


Figure 5. Electric field intensity distributions and surface current distributions of the proposed MA with different width l of metallic bamboo joint structure: (a) $l=2.0\text{mm}$, (b) $l=4.0\text{mm}$, and (c) $l=6.0\text{mm}$.

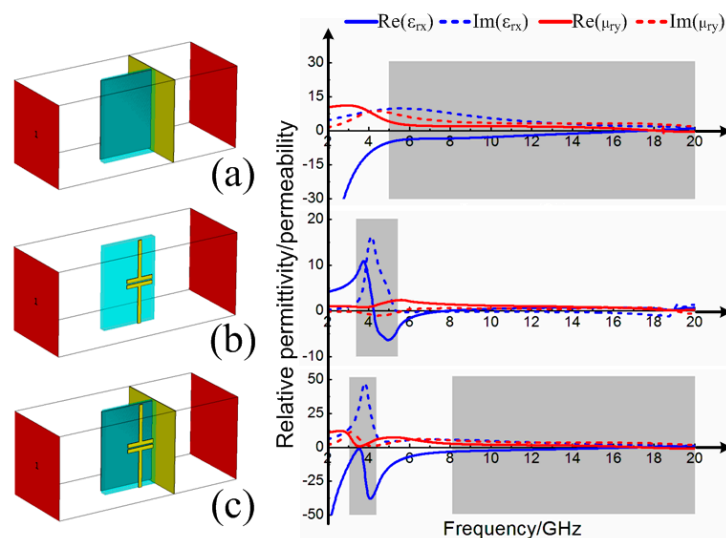


Figure 6. Constitutive parameters of (a) the three-dimensional resistive MA, (b) the MRs of bamboo joint

structure, (c) the three-dimensional resistive MA loaded with MR.

4. Multi-unit Combinations

Three-dimensional resistive MAs loaded with MRs succeeded in separating partial absorption band to lower frequency for the reconfigurable broadband electromagnetic wave absorption. Due to the strong resonance inspired by the MRs, highly effective absorption band was achieved at lower frequency also companies with the discontinuousness absorption at the middle frequencies. To eliminate the absorption trough, the multi-unit combination of the proposed MA to construct the continuously broadband absorption was also proposed. However, it should be noted that the combination of multi-unit still followed the original duty ratio to keep the original light weight characteristic. In the process of combination design, we respectively selected the combination of two-units, three-units and four-units to discuss the broadband absorption performance. Figure 7a firstly showed the combination of two units. The different width of bamboo joint $l=1.0$ and 2.0mm , respectively. And the simulated result showed that the combination of two-units can exhibit stair-stepping broadband absorption performance with the efficiency more than 70% from 3.4 to 6.5GHz and 90% from 6.5 to 21.0GHz. Figure 7b also showed the combination of three units with different width of bamboo joint $l=1.0$, 2.0 and 3.0mm . The simulated result showed that the three-units can exhibit the broadband absorption with the efficiency more than 70% from 3.2 to 6.7GHz and 90% from 6.7 to 21.0GHz. Furthermore, the combination of four-units with the different width of bamboo joint width $l=1.0$, 2.0 , 3.0 and 4.0mm was shown in Figure 7c, the continuously broadband absorption can be further expanded to lower frequency with the efficiency more than 70% from 3.0 to 6.6GHz and 90% from 6.6 to 20.8GHz. Compared with the original resistive MA, the proposed combined MA effectively enhanced the broadband absorption of lower frequency at the sacrifice of high absorbing efficiency, while keeping the broadband absorption at rest frequency unchanged. Meanwhile, we also calculated the limited bandwidth ratio for the combination of two-units, three-units, and four-units during the frequency band of 1.0-26.0GHz. The calculated results of the proposed three models were still the same with the former resistive MA which further verified that the fundamental absorbing principle and total absorbing efficiency during the operating frequencies was still unchanged. Thus, three-dimensional resistive MAs loaded with MRs can exhibit more flexible and various broadband absorption performance according to our expectation.

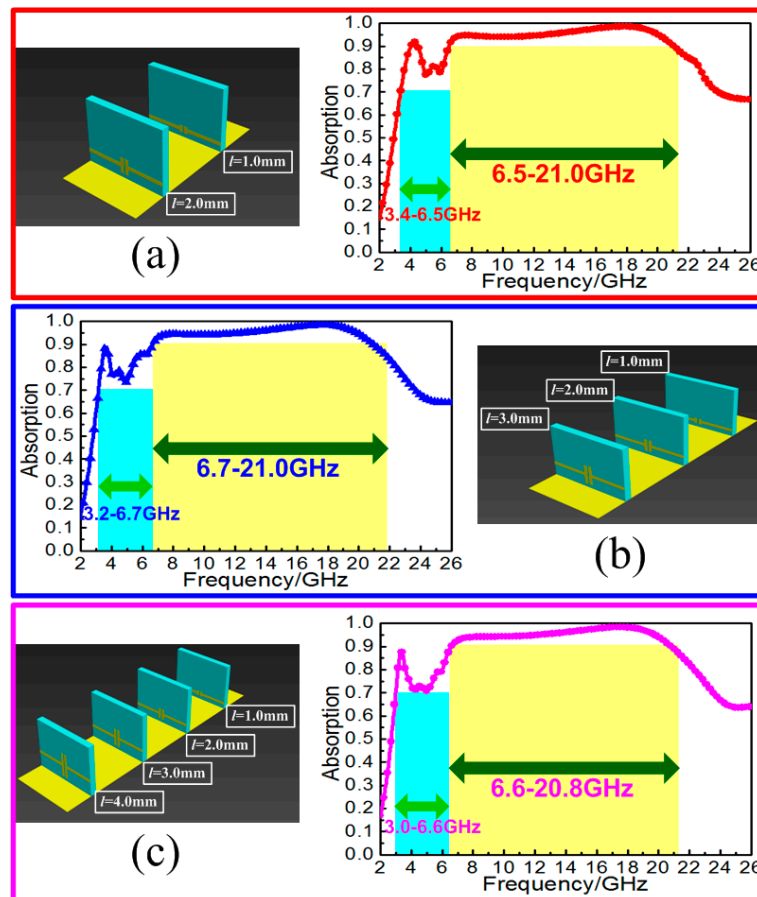


Figure 7. Structure diagram and simulated absorption spectra for the combination of (a) two-units, (b) three-units, and (c) four-units.

5. Measurements and Discussions

To fabricate the combination of aforementioned three samples, the screen printing technology was firstly introduced here to fabricate the resistive patch. The rectangular F4B3 substrate as a group consist of 27 unit cell in the same plane were printed with metallic bamboo joint structure of different width $l=1.0$, 2.0, 3.0 and 4.0mm. Then, the resistive patches were adhered to the other side of the F4B3 substrate periodically, and the basic components of the proposed MA were achieved. Meanwhile, the implemented $297 \times 297 \text{mm}^2$ -sized copper plate with foam-fabricated card slots was also fabricated here. When two, three and four kinds of the MA components with different width of metallic bamboo joint structure were inserted to the card slots according the periodic configuration, the combination of two-units, three-units, and four-units were finally achieved.

The experimental measurements of the fabricated three samples were performed by the arch measurement system in a microwave anechoic chamber. The system is based on an Agilent E8363B network analyzer with two pair of broadband antenna horns respectively working in the frequency bands of 2-8GHz, 8-12GHz, and 12-20GHz. The agreement between simulations and measurements indicated that resistive MAs loaded with MRs can effectively enhance the lower-frequency

absorption with almost no change of the absorbing structure and areal density.

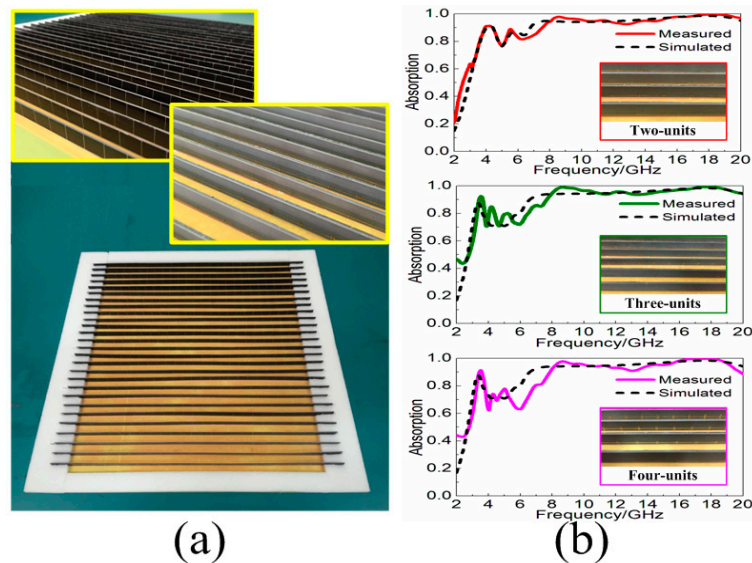


Figure 8. (a) Fabricated samples of the combined MAs in figure 7. (b) Measured and simulated absorption spectra for the combination of two-units, three-units, and four-units.

6. Conclusions

In conclusion, we showed that resistive MA loaded with MRs can further optimized the broadband absorption for the enhancement of lower-frequency absorption. In the example of implementation, we loaded the metallic bamboo joint structures to the three-dimensional resistive MA. Simulation showed that the partial absorption band of the proposed MA was separated to lower frequency, while the rest absorption band was unchanged. Meanwhile, the separated absorption band can be adjusted with different size of MRs. Then, after combining the multi-unit of the proposed MA, the stair-stepping broadband absorption was also achieved. During the reconfigured process, the simple absorption principle and light-weight characteristic were always unaffected. At last, three samples were fabricated. The good agreement between experimental results and simulations demonstrated that resistive MAs loaded with MRs provided an effective way for further enhancement of lower-frequency absorption. Never have attempts concentrated on the reconfiguration of the broadband absorption for further enhancement of lower-frequency absorption, nor have resistive MA loaded with MRs was designed in three-dimensional construction. Thus, it is worthy to expect that several applications can be referenced from the proposed methods.

Acknowledgements: The authors are grateful to the support from the National Natural Science Foundation of China (Grant Nos. 61471388 and 61671467), the China Postdoctoral Science Foundation (Grant No. 2015M572561), the Foundation for the Author of National Excellent Doctoral Dissertation of the People's Republic of China under (Grant No. 201242), and the Shanxi Province Scientific and Technology Innovation Team Foundation of China (Grant No. 2014KCT-05).

Author Contributions: Y.S. and Y.P. conceived the idea and did the numerical simulations. Y.S. and Y.P. fabricated the samples and conducted the measurements. Y.S., J.Z., Y.P., J.W., H.M. and S.Q. gave the theoretical analysis and guiding advice. Y.S. achieved the manuscript, and all of other authors reviewed the manuscript.

Conflicts of Interest: The authors declare no conflict of interest.

References

1. Kundtz, N.; Smith, D. R. Extreme-angle broadband metamaterial lens. *Nat. Mater.* **2010**, *9*, 129-132. [[CrossRef](#)] [[PubMed](#)]
2. Scarborough, C.P.; Jiang, Z.H.; Werner, D.H.; Rivero-Baleine, C.; Drake, C. Experimental demonstration of an isotropic metamaterial super lens with negative unity permeability at 8.5 MHz. *Appl. Phys. Lett.* **2012**, *101*, 014101. [[CrossRef](#)] [[PubMed](#)]
3. Jiang, W.X.; Ge, S.; Han, T.; Zhang, S.; Mehmood, M.Q.; Qiu, C.W.; Cui, T.J. Shaping 3D path of electromagnetic waves using gradient-refractive-index metamaterials. *Adv. Sci.* **2016**, *3*, 1600022. [[CrossRef](#)] [[PubMed](#)]
4. Schurig, D.; Mock, J.J.; Justice, B.J.; Cummer, S.A.; Pendry, J.B.; Starr, A.F.; Smith, D.R. Metamaterial electromagnetic cloak at microwave frequencies. *Science* **2006**, *314*, 977-980. [[CrossRef](#)] [[PubMed](#)]
5. Ma, H.; Qu, S.; Xu, Z.; Wang, J. The open cloak. *Appl. Phys. Lett.* **2009**, *94*, 103501. [[CrossRef](#)] [[PubMed](#)]
6. Jiang, W.X.; Luo, C.Y.; Mei, Z.L.; Cui T J. An ultrathin but nearly perfect direct current electric cloak. *Appl. Phys. Lett.* **2013**, *102*, 014102. [[CrossRef](#)] [[PubMed](#)]
7. Landy, N.I.; Sajuyigbe, S.; Mock, J.J.; Smith, D.R.; Padilla, W. J. Perfect metamaterial absorber. *Phys. Rev. Lett.* **100**, 207402, 2008. [[CrossRef](#)] [[PubMed](#)]
8. Tao, H.; Bingham, C.M.; Pilon, D.; Fan, K.; Strikwerda, A.C.; Shrekenhamer, D.; Padilla, W.J.; Zhang, X.; Averitt, R.D. A dual band terahertz metamaterial absorber. *J. Phys. D: Appl. Phys.* **2010**, *43*, 225102. [[CrossRef](#)] [[PubMed](#)]
9. Zhao, J.; Cheng, Q.; Chen, J.; Qi, M.; Jiang, W.; Cui, T. A tunable metamaterial absorber using varactor diodes. *New J. Phys.* **2013**, *15*, 043049. [[CrossRef](#)] [[PubMed](#)]
10. Zheng, H.; Jin, X.; Park, J.; Lu Y.; Rhee J.; Jang W.; Cheong, H.; Lee, Y. Tunable dual-band perfect absorbers based on extraordinary optical transmission and Fabry-Perot cavity resonance. *Opt. Express* **2012**, *20*, 24002-24009. [[CrossRef](#)] [[PubMed](#)]
11. Yuan, H.; Zhu, B.; Feng, Y. A frequency and bandwidth tunable metamaterial absorber in x-band. *J. Appl. Phys.* **2015**, *117*, 173103. [[CrossRef](#)] [[PubMed](#)]
12. Wang, B.; Wang, G. Quad-Band terahertz absorber based on a simple design of metamaterial resonator. *IEEE Photon. J.* **2016**, *8*, 5502408. [[CrossRef](#)] [[PubMed](#)]
13. Zhang, X.; Liu, H.; Li, L. Tri-band miniaturized wide-angle and polarization-insensitive metasurface for ambient energy harvesting. *Appl. Phys. Lett.* **2017**, *111*, 071902. [[CrossRef](#)] [[PubMed](#)]
14. Huang, L.; Chowdhury, D.R.; Ramani, S.; Reiten, M.T.; Luo, S.N.; Taylor, A.J.;

Chen, H.T. Experimental demonstration of terahertz metamaterial absorbers with a broad and flat high absorption band. *Opt. Lett.* **2012**, *37*, 154-156. [[CrossRef](#)] [[PubMed](#)]

15. Shen, Y.; Pei, Z.; Pang, Y.; Wang, J.; Zhang, A.; Qu, S. Phase random metasurfaces for broadband wide-angle radar cross section reduction. *Micro. Opt. Tech. Lett.* **2015**, *57*, 2813-2819. [[CrossRef](#)] [[PubMed](#)]

16. Ding, F.; Cui, Y.; Ge, X.; Jin, Y.; He, S. Ultra-broadband microwave metamaterial absorber. *Appl. Phys. Lett.* **2012**, *100*, 103506. [[CrossRef](#)] [[PubMed](#)]

17. Pang, Y.; Wang, J.; Ma H.; Feng, M.; Li, Y.; Xu, Z.; Xia, S.; Qu, S. Spatial k-dispersion engineering of spoof surface plasmon polaritons for customized absorption. *Sci. Rep.* **2016**, *6*, 29429. [[CrossRef](#)] [[PubMed](#)]

18. Jiang, W.; Ma, Y.; Yuan, J.; Yin, G.; Wu, W.; He, S. Deformable broadband metamaterial absorbers engineered with an analytical spatial Kramers-Kronig permittivity profile. *Laser Photon. Rev.* **2017**, *11*, 1600253. [[CrossRef](#)] [[PubMed](#)]

19. Ye, D.; Wang, Z.; Xu, K.; Li, H.; Huangfu, J.; Wang, Z.; Ran, L. Ultrawideband dispersion control of a metamaterial surface for perfectly-matched-layer-like absorption. *Phys. Rev. Lett.* **2013**, *111*, 187402. [[CrossRef](#)] [[PubMed](#)]

20. Li, S.; Gao, J.; Cao, X.; Li, W.; Zhang, Z.; Zhang, D. Wideband, thin, and polarization-insensitive perfect absorber based the double octagonal rings metamaterials and lumped resistances. *J. Appl. Phys.* **2014**, *116*, 043710. [[CrossRef](#)] [[PubMed](#)]

21. Yuan, W.; Cheng, Y. Low-frequency and broadband metamaterial absorber based on lumped elements: design, characterization and experiment. *Appl. Phys. A* **2014**, *117*, 1915-1921. [[CrossRef](#)] [[PubMed](#)]

22. Kim, Y.; Hwang, J.; Yoo, Y.; Khuyen, B.; Rhee, J.; Chen, X.; Lee, Y. Ultrathin microwave metamaterial absorber utilizing embedded resistors. *J. Phys. D: Appl. Phys.* **2017**, *50*, 112960. [[CrossRef](#)] [[PubMed](#)]

23. Sun, L.; Cheng, H.; Zhou, Y.; Wang, J. Broadband metamaterial absorber based on coupling resistive frequency selective surface. *Opt. Express* **2012**, *20*, 4675-4680. [[CrossRef](#)] [[PubMed](#)]

24. Pang, Y.; Cheng, H.; Zhou, Y.; Li, Z.; Wang, J. Ultrathin and broadband high impedance surface absorbers based on metamaterial substrates. *Opt. Express* **2012**, *20*, 12515-12520. [[CrossRef](#)] [[PubMed](#)]

25. Shang, Y.; Shen, Z.; Xiao, S. On the design of single-layer circuit analog absorber using double-square-loop array. *IEEE Trans. Antennas Propag.* **2013**, *61*, 6022-6029. [[CrossRef](#)] [[PubMed](#)]

26. Shen, Y.; Pei, Z.; Pang, Y.; Wang, J.; Zhang, A.; Qu, S. An extremely wideband and lightweight metamaterial absorber. *J. Appl. Phys.* **2015**, *117*, 224503. [[CrossRef](#)] [[PubMed](#)]

27. Shen, Y.; Pang, Y.; Wang, J.; Ma, H.; Pei, Z.; Qu, S. Origami-inspired metamaterial absorbers for improving the larger-incident angle absorption. *J. Phys. D: Appl. Phys.* **2015**, *48*, 445008. [[CrossRef](#)] [[PubMed](#)]

28. Zhang, C.; Cheng, Q.; Yang, J.; Zhao, J.; Cui, T. Broadband metamaterial for optical transparency and microwave absorption. *Appl. Phys. Lett.* **2017**, *110*, 143511.

[[CrossRef](#)] [[PubMed](#)]

29. Hu, D.; Cao, J.; Li, W.; Zhang, C.; Wu, T.; Li, Q.; Chen, Z.; Wang, Y.; Guan, J. Optically transparent broadband microwave absorption metamaterial by standing-up closed-ring resonators *Adv. Opt. Mat.* 2017, 3, 1700109. [[CrossRef](#)] [[PubMed](#)]
30. Rozanov, K. N. Ultimate thickness to bandwidth ratio of radar absorbers. *IEEE Trans. Antennas Propag.* 2000, 48, 1230-1234. [[CrossRef](#)] [[PubMed](#)]